Comparative photochemistry of ring-substituted half-sandwich tetracarbonylvanadium complexes in low-temperature matrices at ca. 12 K

Antony J. Rest, Max Herberhold, and Matthias Schrepfermann

Organometallics, **1992**, 11 (11), 3646-3658• DOI: 10.1021/om00059a030 • Publication Date (Web): 01 May 2002

Comparative Photochemistry of Ring-Substituted Half-Sandwich Tetracarbonylvanadium Complexes in Low-Temperature Matrices at ca. 12 K

Antony J. Rest*

Department of Chemistry, The University, Southampton SO9 5NH, United Kingdom

Max Herberhold and Matthias Schrepfermann

Laboratorium für Anorganische Chemie, Universität Bayreuth, Postfach 10 12 51, D-8580 Bayreuth, Germany

Received April 23, 1992

Infrared spectroscopic evidence is presented showing that photolysis of a variety of ring-substituted half-sandwich tetracarbonylvanadium complexes (ring: η^5-C_5Me_5, η^5-C_5H_4Me, η^5-indenyl, η^5-C_5Cl_5) in Ar and CH_4 matrices at high dilution at ca. 12 K affords reversible CO ejection and partial ring dechelation. For the η^5-C_5H_4Me and η^5-C_5Cl_5 compounds, further photolysis led to dicarbonyl species. In N_2 matrices reversible ring dechelation was also observed but the CO loss species reacted with N_2 to yield mono- and bis(dinitrogen) species. In CO matrices reversible ring dechelation was still observed but there was no evidence for CO uptake by these species resulting in complete ejection of the cyclopentadienyl rings. In O_2 matrices photolysis of (η^5-C_5Me_5)$V(CO)_4$ led to the formation of (η^5-C_5Me_5)$V(CO)_3(O_2)$ with a side-on bonded O_2 ligand, as confirmed using an $^{18}O_2$ matrix. In Ar matrices doped with H_2S and tetrahydrofuran (THF), there was no evidence for uptake of the donor ligands. In poly(vinyl chloride) films photolysis of (η^5-C_5Me_5)$V(CO)_4$ also gave both the CO loss and the ring dechelation product at 12 K, but as the film was warmed, bands were observed which were consistent with the formation of (η^5-C_5Me_5)$V(CO)_3$(THF). The photoreactions at 12 K are discussed and compared to those of (η^5-C_5H_5)$V(CO)_4$ and related to the preparative and mechanistic thermal and photochemical reactions at ambient temperatures. It is apparent that more credence should be given to ring dechelation/ring slippage pathways when reaction mechanisms are discussed.

Introduction

Many (η^5-cyclopentadienyl)tetracarbonylvanadium compounds, especially those of the pentamethylcyclopentadienyl derivative $Cp^*V(CO)_4$ (1; $Cp^* = \eta^5$-C_5Me_5), undergo a variety of thermal and photochemical reactions. The oxidative decarbonylation by elemental halogens X_2 (X_2 = Cl_2, Br_2, I_2) leads to V(IV) complexes of the type Cp^*VX_3 which can be oxidized[1] to yield the corresponding V(V) oxo dihalides, Cp^*VOX_2 (eq 1). The latter complexes can also be obtained by the reaction of $Cp^*V(CO)_4$ with the hydrogen halides HX (X = F, Cl, Br, I) in tetrahydrofuran (THF) solutions. Extended reaction times led to the formation of dimeric compounds (eq 2).

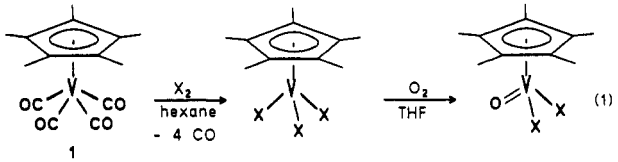

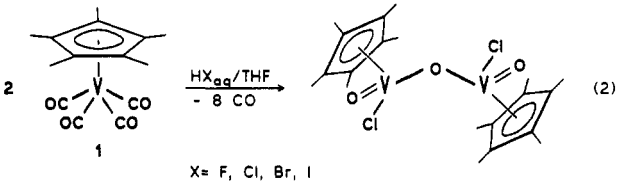

The reactions of either dioxygen[1,2] or oxygen sources such as Me_3NO,[3] C_5H_5NO,[4] and N_2O[5,6] with $Cp^*V(CO)_4$ or $CpV(CO)_4$ and a reaction of Cp^*VOCl_2 with Ag_2CO_3[7] led to a variety of organometallic oxo complexes containing both terminal and bridging oxo ligands: e.g., [(μ-η^3-Cp^*O_3)$V(O)]_2$,[2] $Cp^*_3V_4O_9$,[1] $[Cp^*V(O)(\mu\text{-}O)]_3$,[7] $Cp^*_4V_4(\mu_2\text{-}O)_6$,[6] $Cp_4V_4(\mu_3\text{-}O)_4$ and $Cp_5(O)V_6(\mu_3\text{-}O)_8$,[4] $Cp_5V_5(\mu_3\text{-}O)_6$,[5,8] $Cp_6V_6(\mu_3\text{-}O)_8$, and $Cp_{14}V_{16}O_{24}$.[3]

The photochemically induced reactions of various $Cp^\#V(CO)_4$ complexes ($Cp^\#$, ring-substituted cyclopentadienyl ligands) with donor ligands (D), e.g. chalcogens,[9,10] SR_2 (R = H, Me),[11] mono- and bidentate phosphines,[12-18] and amines,[19,20] in tetrahydrofuran are pro-

* Address correspondence to this author.

(1) Herberhold, M.; Kremnitz, W.; Kuhnlein, M. *Z. Naturforsch.* **1987**, *42B*, 1520.
(2) Bottomley, F.; Magill, C. P.; White, P. S. *J. Am. Chem. Soc.* **1989**, *111*, 3070.
(3) Bottomley, F.; Paez, D. E.; White, P. S. *J. Am. Chem. Soc.* **1985**, *107*, 7226.
(4) Bottomley, F.; Drummond, D. F.; Paez, D. E.; White, P. S. *J. Chem. Soc., Chem. Commun.* **1986**, 1752.
(5) Bottomley, F.; Paez, D. E.; White, P. S. *J. Am. Chem. Soc.* **1982**, *104*, 5651.
(6) Bottomley, F.; Magill, C. P.; Zhao, B. *Organometallics* **1990**, *9*, 1700.
(7) Bottomley, F.; Sutin, L. *J. Chem. Soc., Chem. Commun.* **1987**, 1112.
(8) Bottomley, F.; Grein, F. *Inorg. Chem.* **1982**, *21*, 4170.
(9) Herberhold, M.; Kuhnlein, M. *New J. Chem.* **1988**, *12*, 357.
(10) Herberhold, M.; Kuhnlein, M.; Schrepfermann, M.; Ziegler, M. L.; Nuber, B. *J. Organomet. Chem.* **1990**, *398*, 259.
(11) Herberhold, M.; Kuhnlein, M.; Rheingold, A. L.; *J. Organomet. Chem.* **1990**, *383*, 71.
(12) Tsumura, R.; Hagihara, N. *Bull. Chem. Soc. Jpn.* **1965**, *38*, 1901.
(13) Kinney, R. J.; Jones, W. D.; Bergmann, R. G. *J. Am. Chem. Soc.* **1978**, *100*, 7902.
(14) Alway, D. G.; Barnett, K. W. *Inorg. Chem.* **1980**, *19*, 779.
(15) Fischer, E. O.; Schneider, R. J. *Angew. Chem., Int. Ed. Engl.* **1968**, *6*, 569.
(16) Fischer, E. O.; Louis, E.; Schneider, R. J. *Angew. Chem., Int. Ed. Engl.* **1969**, *7*, 136.
(17) Rehder, D.; Dahlenburg, L.; Müller, I. *J. Organomet. Chem.* **1976**, *122*, 53.
(18) Müller, I.; Rehder, D. *J. Organomet. Chem.* **1977**, *139*, 293.
(19) Woitha, C.; Rehder, D. *J. Organomet. Chem.* **1988**, *353*, 315.
(20) Hoch, M.; Rehder, D. *Inorg. Chim. Acta* **1986**, *115*, L23.

0276-7333/92/2311-3646$03.00/0

posed to proceed via the thermally labile $Cp^{\#}V(CO)_3(THF)$ complex which can in fact be isolated at low temperatures:[19]

$$Cp^{\#}V(CO)_4 \xrightarrow{h\nu} [Cp^{\#}V(CO)_4]^* \quad (3)$$

$$[Cp^{\#}V(CO)_4]^* \rightarrow Cp^{\#}V(CO)_3 + CO \quad (4)$$

$$CpV(CO)_3 + THF \rightarrow CpV(CO)_3(THF) \quad (5)$$

$$CpV(CO)_3(THF) + D \rightarrow CpV(CO)_3D + THF \quad (6)$$

where $[Cp^{\#}V(CO)_4]^*$ describes an excited-state species.

Matrix isolation studies afford the means to trap and characterize the unstable species proposed as intermediates in the reactions shown above.[21] In this paper we present a study of the comparative photochemistry of the ring-substituted half-sandwich tetracarbonylvanadium complexes **1–5** in inert (Ar, CH_4), reactive (N_2, CO, O_2), and doped (H_2S in Ar, THF in Ar) matrices and in poly(vinyl chloride) (PVC) films at ca. 12 K. This work extends the results on $(\eta^5\text{-}C_5H_5)V(CO)_4$ (**3**), which have been reported previously.[22,23]

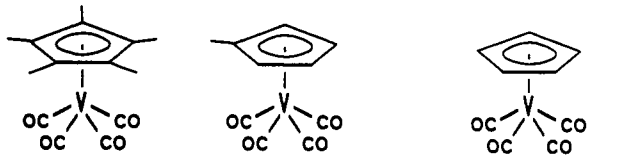

$(\eta^5\text{-}C_5Me_5)V(CO)_4$ (1) $(\eta^5\text{-}C_5H_4Me)V(CO)_4$ (2) $(\eta^5\text{-}C_5H_5)V(CO)_4$ (3)

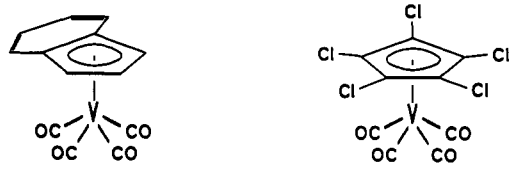

$(\eta^5\text{-indenyl})V(CO)_4$ (4) $(\eta^5\text{-}C_5Cl_5)V(CO)_4$ (5)

Experimental Section

The equipment for matrix isolation studies at Southampton (Air Products and Chemicals Inc., closed cycle He refrigerator (Displex CSW-202), spectrometers, medium-pressure Hg arc (Phillips HPK 125 W), and filters for wavelength-selective photolysis) have been described elsewhere.[24]

The Perkin-Elmer 983G IR spectrometer was operated in double-beam ratio recording mode at a resolution of 1 cm with air as the reference. Spectra (single scans were adequate) were recorded in % *T* mode, converted to absorbance mode for subtraction, and then converted back to % *T* mode, using the Perkin-Elmer 3600 Data Station, for presentation. The intensities of the bands were measured using the integration software package of the Perkin-Elmer Data Station after the conversion of bands from % *T* to absorbance modes. The errors in these computer-assisted calculations should be less than 5%.

The samples for the matrix isolation experiments were freshly prepared according to literature procedures and stored in sealed glass tubes under argon in a deep freeze. $(\eta^5\text{-}C_5Me_5)V(CO)_4$ (**1**)[1,25] and $(\eta^5\text{-}C_5H_4Me)V(CO)_4$ (**2**)[1] were purified by vacuum sublimation at 10^{-3} Torr; $(\eta^5\text{-indenyl})V(CO)_4$ (**4**)[25] and $(\eta^5\text{-}C_5Cl_5)V(CO)_4$ (**5**)[26] were chromatographed twice over SiO_2 using hexane as the eluent in order to remove the unreacted cyclopentadienes (indene, hexachlorocyclopentadiene).

The gases for the matrix isolation experiments (Ar, CH_4, CO, N_2, O_2) were all BOC Research Grade (>99.999%). $^{18}O_2$ (>97%) was obtained from Cea-Oris, Bureau Des Isotopes Stables (B.P. 21-91190, Gif-Sur-Yvette, France). All gases were used without further purification.

Gas mixtures were prepared using a vacuum line and standard manometric techniques. The dopants THF (BDH Limited, Poole, England; <0.03% water, degassed by five freeze–pump–thaw cycles) and H_2S (BOC Commercial grade) were also used without further purification.

All the samples studied were deposited using the slow spray-on technique. The complex was placed in a suitable deposition head, and if necessary, the temperature was reduced or raised using an appropriate low-temperature bath or an induction heater.

The matrix gas, introduced from a prefilled detachable 1-L bulb via a capillary line, was cocondensed with the sample onto the cold spectroscopic window. The gas flow rate was adjusted using a precision needle valve (B-MF-1-V-2PH-TCD) manufactured by Negretti and Zambra (Aviation) Ltd.

Careful selection of sample temperature, gas flow rate, and deposition time was necessary to obtain a satisfactory matrix quality, and progress was monitored at suitable stages during deposition (Table I). Polymer films of $(\eta^5\text{-}C_5Me_5)V(CO)_4$ (**1**) in poly(vinyl chloride) were prepared in the dark under N_2, as described previously.[27] Specific selective photolyses within narrow bandwidth ranges were achieved by combinations of absorbing materials described in Table II.

Table I. Deposition Temperatures and Times for the Compounds Investigated by Matrix Isolation

sample	deposition temp (°C)	deposition time (min)
$(\eta^5\text{-}C_5Me_5)V(CO)_4$ (1)	25	90
$(\eta^5\text{-}C_5H_4Me)V(CO)_4$ (2)	−10	60
$(\eta^5\text{-indenyl})V(CO)_4$ (4)	35	120
$(\eta^5\text{-}C_5Cl_5)V(CO)_4$ (5)	25	60

Table II. Filter Materials Used in Conjunction with the Medium-Pressure Mercury Lamp

filter	wavelength (nm)	description
A	$\lambda > 430$	Corning glass color filter, CS 3–74
B	$320 < \lambda < 390$	Corning glass color filter, CS 7–60
C	$\lambda > 510$	Corning glass color filter, CS 3–70
D	$380 < \lambda < 440$	Corion interference filter, P70-400-S-1339
E	$290 < \lambda < 370$ and $\lambda > 550$	quartz gas cell (path length 25 mm) containing Br_2 (300 Torr) + Pyrex disk (3 mm thick)
F	$230 < \lambda < 280$	quartz gas cell (path length 25 mm) containing Cl_2 (2 atm) + Corning color filter CS 7–54 (3 mm thick)

Table III. Electronic Absorption Bands of Complexes 1–5 Isolated at High Dilution (1:2000–1:5000) in Argon Matrices

complex	assigned transitions (nm): charge transfer[a]			d–d[b]
$(\eta^5\text{-}C_5Me_5)V(CO)_4$ (1)	288	306	364	410
$(\eta^5\text{-}C_5H_4Me)V(CO)_4$ (2)	286	308	366	416
$(\eta^5\text{-}C_5H_5)V(CO)_4$ (3)	280		364	410
$(\eta^5\text{-indenyl})V(CO)_4$ (4)		306	362	
$(\eta^5\text{-}C_5Cl_5)V(CO)_4$ (5)	289	304	386	436

[a] Absorbance in the UV spectrum. [b] Absorbance in the visible spectrum.

Results

Electronic Absorption Spectra. The UV–visible absorption spectra of complexes **1–5** in a variety of matrices

(21) (a) Barnes, A. J., Gaufrès, R., Müller, A., Orville-Thomas, W. J., Eds. *Matrix Isolation Spectroscopy*; NATO Advanced Study Institutes Series C; Reidel, D.: Dordrecht, The Netherlands, 1981; Chapter 1. (b) Hitam, R. B.; Mahmoud, K. A.; Rest, A. J. *Coord. Chem. Rev.* **1984**, *55*, 1. (c) Perutz, R. N. *Chem. Rev.* **1985**, *85*, 97.

(22) Hitam, R. B.; Rest, A. J. *Organometallics* **1989**, *8*, 1598.

(23) Haward, M. T.; George, M. W.; Howdle, S. M.; Poliakoff, M. *J. Chem. Soc., Chem. Commun.* **1990**, 913.

(24) Mahmoud, K. A.; Narayanaswamy, R.; Rest, A. J. *J. Chem. Soc., Dalton Trans.* **1981**, 2199.

(25) Hoch, M.; Rehder, D.; Duch, A. *Inorg. Chem.* **1986**, *25*, 2907.

(26) Priebsch, W.; Hoch, M.; Rehder, D. *Chem. Ber.* **1988**, *121*, 1971.

(27) Hooker, R. H.; Rest, A. J. *Appl. Organomet. Chem.* **1990**, *4*, 141.

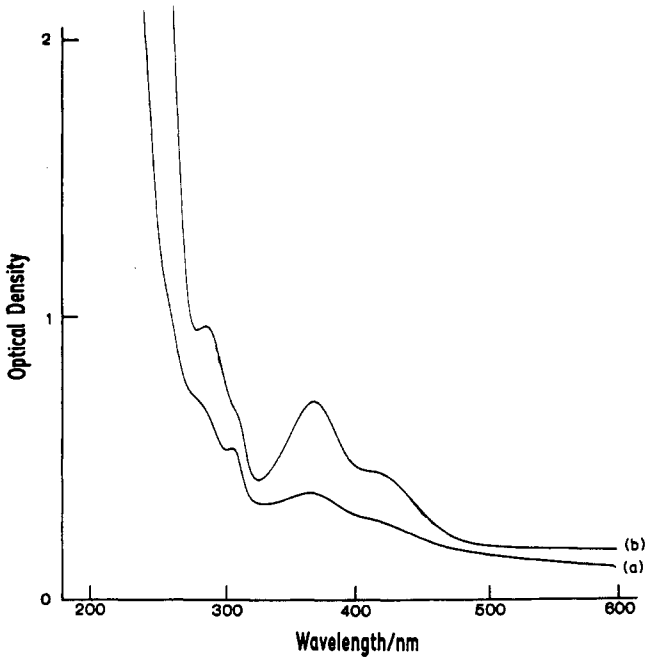

Figure 1. Electronic absorption spectra from an experiment with (a) $(\eta^5\text{-}C_5Me_5)V(CO)_4$ (1) and (b) $(\eta^5\text{-}C_5H_4Me)V(CO)_4$ (2) isolated at high dilution in an Ar matrix at ca. 12 K (Perkin-Elmer Lambda 7).

showed marked similarities. Typical spectra for 1 and 2 at high dilution in Ar matrices are shown in Figure 1.

The long-wavelength bands may reasonably be assigned as d → d transitions while the bands at high energy are likely to be V → π*(CO) charge-transfer transitions.[28] The frequencies of the electronic absorption bands of complexes 1–5 are summarized in Table III.

The photolysis of the isolated half-sandwich compounds used specific filters to match the irradiation wavelength with the electronic absorption band maxima of the complexes.

Photolyses of Complexes 1–5 in Ar and CH_4 Matrices at ca. 12 K. In order to present the work concisely, general photoreactions will be described using a typical complex. Photoreactions specific to particular compounds will be discussed separately in this and the following sections.

The infrared spectrum of $(\eta^5\text{-}C_5Me_5)V(CO)_4$ (1) on deposition showed matrix split terminal CO stretching bands at 2019 and 1920 cm^{-1} expected for the A_1 and E modes, respectively, of a C_{4v} local symmetry $V(CO)_4$ fragment. The appearance of the infrared-inactive B_1 band at 1939 cm^{-1} is indicative of some deviation from strict C_{4v} local symmetry (Figure 2). A good correspondence was found between infrared band positions for hexane solutions and gas matrices (Table IV).

A short period of visible irradiation (filter A, λ > 430 nm) produced new bands at 2140, 2036, 1979, 1959, 1900, and 1880 cm^{-1}. Of these bands, the one at 2140 cm^{-1} corresponds to CO which has been ejected as a result of photolysis but is still close to the metal complex. This photoejected CO is referred to as "free" CO.[29] On further

Table IV. Observed Absorption Bands (cm^{-1}) of Complexes 1–5 in Hexane Solution at 25 °C and in a CH_4 Matrix (Half-Widths in Parentheses) at ca. 12 K

complex	in hexane		in CH_4	
$(\eta^5\text{-}C_5Me_5)V(CO)_4$ (1)	2014	1916	2017 (6)	1919 (11)
$(\eta^5\text{-}C_5H_4Me)V(CO)_4$ (2)	2027	1929	2027 (8)	1929 (21)
$(\eta^5\text{-}C_5H_5)V(CO)_4$ (3)	2029	1935	2030[a]	1931[a]
$(\eta^5\text{-indenyl})V(CO)_4$ (4)	2026	1933	2029 (7)	1934 (16)
$(\eta^5\text{-}C_5Cl_5)V(CO)_4$ (5)	2046	1963	2051 (3)	1966 (10)

[a] Data from ref 22; half-width not given.

irradiation with UV light (filter B, 320 < λ < 390 nm) the new bands grew in intensity, while those of the parent compound 1 decreased. On long-wavelength irradiation (filter C, λ > 510 nm, not illustrated) or on annealing the matrix to ca. 35 K (annealing is a process by which the matrix is allowed to warm and soften, hence allowing unstable species to diffuse through the matrix), an intensity decrease was observed in the band of free CO and in the bands at 1979, 1900, and 1880 cm^{-1} with concomitant increases in the intensities of the bands at 1979, 1900, and 1880 cm^{-1} and increases in the intensities of the parent bands. In contrast to this, the bands at 2036 and 1959 cm^{-1} remained nearly constant (in the case of annealing) or grew slightly in intensity (upon long-wavelength irradiation).

From the behavior (increases/decreases in intensity) of the product bands during various photolyses and annealing, it is possible to identify two different species (species **1a**, 2036, 1959 cm^{-1}; species **1b**, 1979, 1900, 1880 cm^{-1}). The high dilution used (at least 1:2000)[30] and the reversibility of the reactions photochemically and thermally (annealing) rules out the possibility of any polynuclear aggregates, e.g., $Cp^*_2V_2(CO)_5$.

The fact that photogenerated free CO was observed suggests that ejection of CO from the parent complex has occurred, and it seems plausible to formulate one species as $(\eta^5\text{-}C_5Me_5)V(CO)_3$ (**1b**). The band shifts of ca. 40–50 cm^{-1} to lower wavenumbers are consistent with the observations for $(\eta^5\text{-}C_5H_5)V(CO)_3$ (**3b**).[22] It was not possible, however, even using high-energy UV irradiation (filter E, 290 < λ < 370 and λ > 550 nm; or filter F, 230 < λ < 280 nm) to generate the corresponding di- or monocarbonyl species $Cp^*V(CO)_n$ (n = 1, 2) in the matrix. Interestingly, the bands of species **1a** are shifted to higher wavenumbers. It seems reasonable to suggest the formation of a coordinatively unsaturated ring slippage species $(\eta^3\text{-}C_5Me_5)V(CO)_4$ (**1a**), generated by partial dechelation of the hydrocarbon ring. The bands for the analogous complex $(\eta^3\text{-}C_5H_5)V(CO)_4$ (**3a**) proposed in a recent study[22] were shifted to slightly lower wavenumbers (ca. 10 cm^{-1}).

In order to investigate ring dechelation processes and knowing that species **1a** can be generated in high yield using filter A, both the methyl bending region (1430–1340 cm^{-1}) and the range covering the ring skeleton vibrations (1080–900 cm^{-1}) were recorded. The spectra after deposition and 20-min visible irradiation (filter A) are illustrated in Figure 3 together with the difference spectrum. The parent complex 1 exhibited CH_3 bending vibrations at 1390 and 1384 cm^{-1} and one single ring skeleton absorption due to a symmetrically bound $\eta^5\text{-}C_5Me_5$ ligand at 1034 cm^{-1}. The dechelation product $(\eta^3\text{-}C_5Me_5)V(CO)_4$ (**1a**) produced in high yield after visible irradiation only showed a slight shift in the band position of the methyl bending vibrations (1392, 1385 cm^{-1}) and the appearance of a new

(28) Geoffroy, G. L.; Wrighton, M. S. *Organometallic Photochemistry*; Academic Press: New York, 1979.

(29) The initial spectra of 1 and of the other complexes show *two* CO bands at 2149 and 2140 cm^{-1}, which arise from the thermal decompoeition during spray-on. The band at 2149 cm^{-1}, which remains invariant during the experiments of photolyses and annealing, corresponds to CO which is separated from the metal complex whereas the band at 2140 cm^{-1} corresponds to CO in the same cage as the molecules of the metal complex.

(30) As deduced by comparison with previous experiments using samples which were volatile enough to be studied by slow spray-on and using gas mixtures prepared to exact substrate/host ratios using manometric techniques.

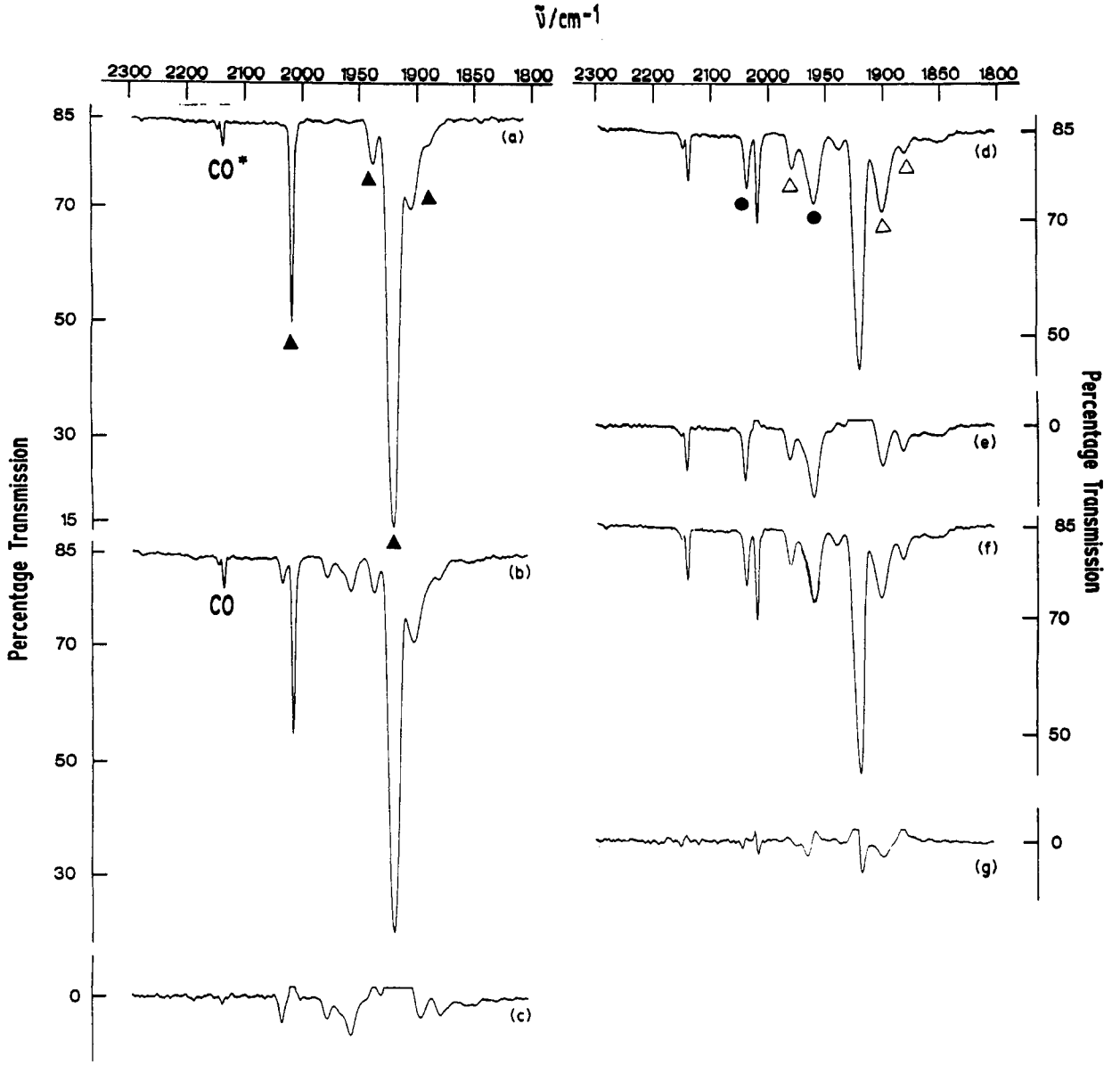

Figure 2. Infrared spectra (Perkin-Elmer 983G) from an experiment with (η^5-C_5Me_5)$V(CO)_4$ (1) isolated at high dilution in an Ar matrix at ca. 12 K: (a) after deposition, (b) after 5-min visible irradiation (filter A), (c) difference spectrum [(b) – (a)], (d) after 5-min UV-irradiation (filter B), (e) difference spectrum [(d) – (b)], (f) after annealing to ca. 35 K, and (g) difference spectrum [(f) – (d)]; (▲) 1 (●) **1a**, and (△) **1b**. (The presence of CO after deposition is due to thermal decomposition and was observed for all complexes.

band pattern with three absorptions at 955, 946, and 935 cm^{-1}. The magnitude of the downward shift and the splitting may be due to the change in the bonding of the ring ligand.

The monomethylcyclopentadienyl complex **2** showed similar behavior in both Ar and CH_4 matrices, except that on extended photolysis (filter B) two further bands at 1951 and 1868 cm^{-1} were revealed by spectral subtraction. In view of the fact that these bands are shifted to lower wavenumbers compared with the bands for the tricarbonyl complex **2b** and diminish together with the absorptions of **2b** on long-wavelength irradiation (filter C) regenerating the parent complex, the new photoproduct may be assigned as the dicarbonyl species (η^5-C_5H_4Me)$V(CO)_2$ (**2c**).

The indenyl complex **4**, in addition to the CO loss product **4b**, and the ring slippage product **4a** showed significant shoulders at 2051 and 1975 cm^{-1}, which alternately increased upon UV irradiation and decreased after long-wavelength photolysis. These shoulders might suggest that an equilibrium process exists in the gas phase (or in solution) which can be quenched at the cold window and that this equilibrium can be perturbed photochemically in gas matrices at cryogenic temperatures.

The η^3-mode in indenyl complexes is preferred because of the aromatization of the benzene part of the ring ligand, i.e., the "indenyl effect":[31]

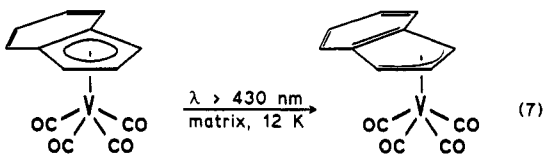

4 **4a** (7)

There are several possibilites for the origins of the shoulder bands: (a) the relative position of the carbonyl ligands to the ring carbons, ring substituents, or ring electrons can cause different V–CO overlapping conditions and thus CO shifts of 5–10 cm^{-1}; (b) investigations of CpNi(NO)[32] have

(31) Merola, J. S.; Kacmarcik, J. T.; Van Engen, D. *J. Am. Chem. Soc.* **1986**, *108*, 329.
(32) Crichton, O.; Rest, A. J. *J. Chem. Soc., Chem. Commun.* **1973**, 407; *J. Chem. Soc., Dalton Trans.* **1977**, 536.

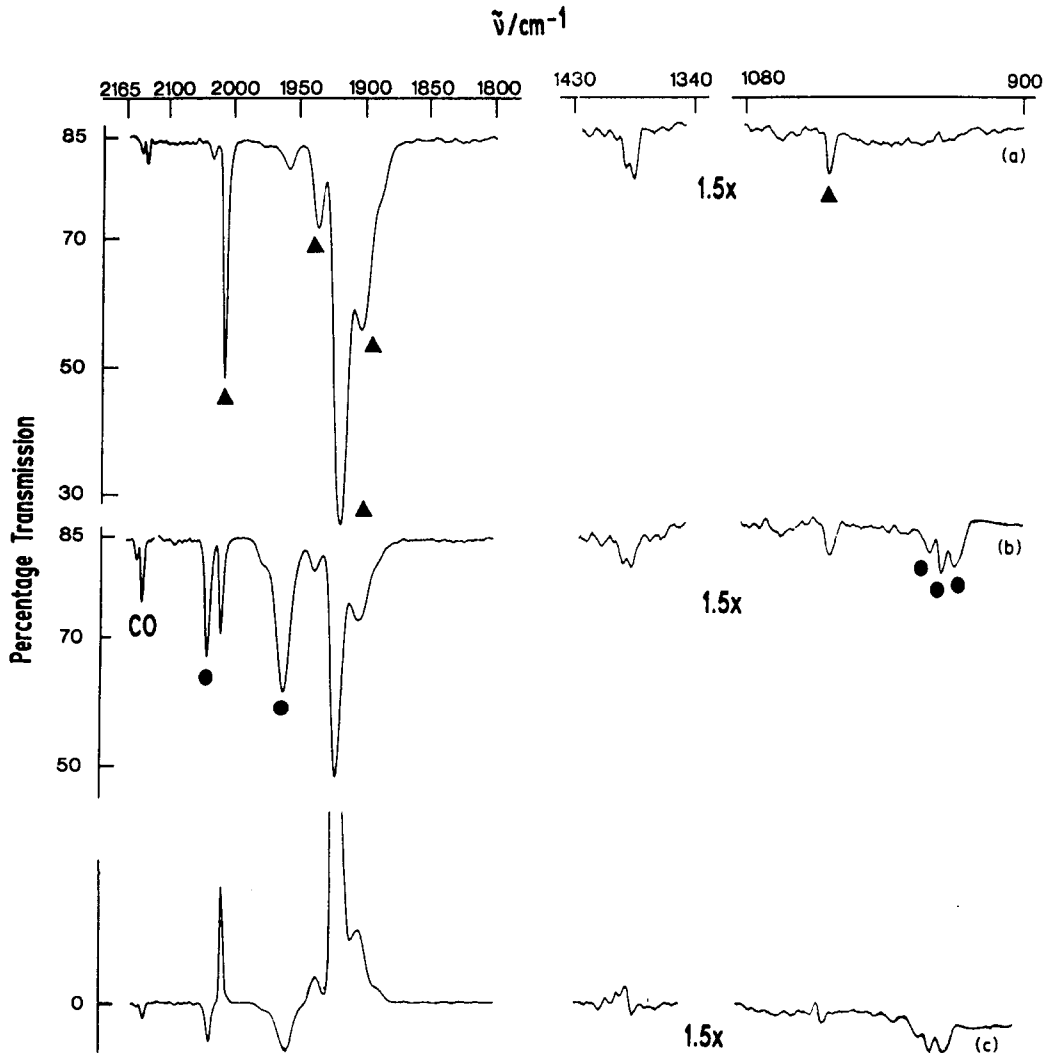

Figure 3. Infrared spectra (Perkin-Elmer 983G) from an experiment with $(\eta^5\text{-}C_5Me_5)V(CO)_4$ (1) isolated at high dilution in an Ar matrix at ca. 12 K: (a) after deposition, (b) after 20-min visible irradiation (filter A), and (c) difference spectrum [(b) − (a)]; (▲) 1 and (●) **1a**.

shown that matrix splitting can be in the range of ca. 10 cm^{-1}, as indicated by the observed ν(NO) absorption bands at 1838, 1834, and 1829 cm^{-1}; (c) previously observed cis–trans—or tub–chair—rearrangements of polyene complexes[33] can be indicated by shifts of about 5 cm^{-1}; (d) processes like the dechelation of a saturated carbon edge of a polyene[33] with a concomitant rearrangement of the metal carbonyl fragment and a recognized agostic interaction to H_{endo} can cause a downward shift of about 2–5 cm^{-1}, due to the increased electron density at the metal center and an increased back-bonding to the CO ligands.

An energetically feasible process caused by UV irradiation would be a downward flip of the allylic carbon C2 resulting in a rearrangement of the $V(CO)_4$ fragment, which is now close to the aromatic ring system.

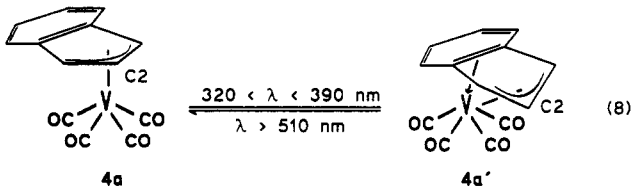

4a 4a′ (8)

The resulting electronic interaction could lead to an increase of the electron density at the metal center with a concomitant increase in the back-donation (V → C) and a decrease in the C–O bond order; i.e., the absorption bands will move to lower wavenumbers. The isomeric species will be designated as **4a′**.

The irradiation of the halogenated complex **5** revealed a marked photolability. Absorption bands attributable to the omnipresent photoproduct $(\eta^3\text{-}C_5Cl_5)V(CO)_4$ (**5a**; 2078, 2034 cm^{-1}) emerged even after a short period of visible irradiation (filter A). Surprisingly, the CO loss species $(\eta^5\text{-}C_5Cl_5)V(CO)_3$ (**5b**; 2023, 1954, 1942 cm^{-1}) and $(\eta^5\text{-}C_5Cl_5)V(CO)_2$ (**5c**; 2001, 1916 cm^{-1}) were then already observable. The concentrations of these species increased after UV irradiation (filter D, 380 < λ < 440 nm) and decreased after long-wavelength photolysis (filter C). A shoulder band at 1905 cm^{-1}, diminishing upon long-wavelength irradiation (filter C) can be tentatively assigned to the monocarbonyl complex $(\eta^5\text{-}C_5Cl_5)V(CO)$ (**5d**). The data for the various parent complexes **1–5** and their photoproducts are given in Table V.

Photolyses of Complexes 1–5 in N_2 Matrices. The infrared spectrum of $(\eta^5\text{-}C_5Me_5)V(CO)_4$ (**1**; 2019, 1920 cm^{-1}) isolated at high dilution in a N_2 matrix (Figure 4) is very similar to those in Ar and CH_4 matrices.

A short period of visible irradiation (filter A) resulted in the appearance of seven new bands at 2192, 2139 (free CO), 2038, 1981, 1960, 1900, and 1865 cm^{-1} together with

(33) Astley, S. T.; Churton, M. P. V.; Hitam, R. B.; Rest, A. J. *J. Chem. Soc., Dalton Trans.* **1990**, 3243.

Table V. Terminal CO Stretching Infrared Band Positions (cm^{-1}) for Complexes 1–5 and their Photoproducts in Ar, CH_4, N_2, and CO Matrices

complex	Ar	CH_4	N_2	CO	complex	Ar	CH_4	N_2	CO
(η^5-C_5Me_5)V(CO)$_4$ (1)	2019	2017	2019	2017	(η^5-C_5H_5)V(CO)$_2$ (3c)[e,f]		1992		
	1939[a]	1938[a]	1940[a]	1937[a]			1894		
	1923[b]		1925[b]		(η^5-C_5H_5)V(CO)$_2$ (3c)[e,g]		1916		
	1920	1921	1920	1919			1814		
	1904[b]	1905[b]	1900[b]	1901[b]	(η^5-C_5H_5)V(CO) (3d)[e]		1830		
	1890[b]		1889[b]	1889[b]	(η^5-C_5H_5)V(CO)$_3$(N_2) (3e)[e]			1996	
(η^3-C_5Me_5)V(CO)$_4$ (1a)	2036	2037	2038	2037				1912	
	1967[b]							*c*	
	1959	1960	1960	1959				2210[d]	
(η^5-C_5Me_5)V(CO)$_3$ (1b)	1979	1979		1979	(η^3-C_5H_5)V(CO)$_5$ (3h)[e]				2055
	1900	1900		1900					1982
	1880	*c*		1880					1946
(η^5-C_5Me_5)V(CO)$_3$(N_2) (1e)			1981		(η^5-indenyl)V(CO)$_4$ (4)	2029	2029	2030	2029
			1900			1957[a]	1957[a]	1958[a]	1957[a]
			c			1935	1934	1936	1934
			2192[d]		(η^3-indenyl)V(CO)$_4$ (4a)	2062	2061	2062	2061
(η^5-C_5Me_5)V(CO)$_2$(N_2)$_2$ (1f)			1969			1986	1988	1989	1995[b]
			1881		(η^3-indenyl)V(CO)$_4$ (4a′)	2051	2051		2054
			2176[d]			1975	1977		*c*
			2151[d]		(η^5-indenyl)V(CO)$_3$ (4b)	1994	1994		
(η^5-C_5H_4Me)V(CO)$_4$ (2)	2028	2027	2030	2028		1916	1917		
	1949[a]	1948	1952[a]	1949[a]		1903	1903		
			1934[b]		(η^5-indenyl)V(CO)$_3$(N_2) (4e)			1995	
	1930	1930	1930	1928				1916	
	1898[b]	1894[b]	1900[b]	1897[b]				1907	
(η^3-C_5H_4Me)V(CO)$_4$ (2a)	2054	2054	2055	2054				2187[d]	
	1979	1981	1981	1979	(η^3-indenyl)V(CO)$_4$(N_2) (4g)			2052	
(η^5-C_5H_4Me)V(CO)$_3$ (2b)	1989	1991		1989				1978	
	1910	1911		*c*				2220[d]	
	1894	1893		*c*	(η^5-C_5Cl_5)V(CO)$_4$ (5)	2051	2051	2052	2051
(η^5-C_5H_4Me)V(CO)$_2$ (2c)	1952	1951				2045[b]	2045[b]	2046[b]	2047[b]
	1865	1868				1988[a]	1988[a]	1988[a]	1988[a]
(η^5-C_5H_4Me)V(CO)$_3$(N_2) (2e)			1991					1970[b]	
			1908			1966	1966	1965	1965
			c			1934[b]	1935[b]	1952[b]	1935[b]
			2211[d]		(η^3-C_5Cl_5)V(CO)$_4$ (5a)	2077	2078	2077	2078
(η^5-C_5H_4Me)V(CO)$_2$(N_2)$_2$ (2f)			1962			2045[b]	2045[b]	2046[b]	2047[b]
			1872			2034	2034	2035	2035
			2190[d]		(η^5-C_5Cl_5)V(CO)$_3$ (5b)	2023	2023		2029
			2182[d]			1953	1954		*c*
(η^5-C_5H_5)V(CO)$_4$ (3)[e]	2034	2030	2033	2030		1942	1942		1947
	2031[b]				(η^5-C_5Cl_5)V(CO)$_2$ (5c)	2001	2002	2003	2003
	1957[a]	1952[a]	1955[a]	1952[a]		1916	1916	*c*	1915
	1939	1931	1938	1930	(η^5-C_5Cl_5)V(CO) (5d)	1905	1905	1904	
	1936[b]		1931[b]		(η^5-C_5Cl_5)V(CO)$_3$(N_2) (5e)			2024	
	1923[b]							1951	
	1906[b]							*c*	
(η^3-C_5H_5)V(CO)$_4$ (3a)[e]	2023	2020	2023	2021				2214[d]	
	1935	1928	*c*	*c*	(η^3-C_5Cl_5)V(CO)$_4$(N_2) (5g)			2085	
(η^5-C_5H_5)V(CO)$_3$ (3b)[e]	1964	1953						2052	
	1902	1887						2231[d]	
	1867	1859							
		1856[b]							

[a] IR-inactive band. [b] Matrix-split band. [c] Obscured by overlapping band of another photoproduct or low intensity due to low abundance. [d] ν(NN). [e] Data from ref 22. [f] Planar geometry. [g] Pyramidal geometry.

two shoulders at ca. 1970 and 1880 cm^{-1}, at the expense of the parent complex. Ultraviolet irradiation (filter B) caused all the new bands to gain intensity, and the two shoulders resolved into absorption bands at 1969 and 1881 cm^{-1}. In addition to this, the high-wavenumber band at 2192 cm^{-1} seemed to become broader and another band at 2151 cm^{-1} gradually appeared. On further long-wavelength irradiation (filter C), the new bands decreased while the absorptions at 2038 and 1960 cm^{-1} slightly increased. The band at 2192 cm^{-1} together with the now clearly separated shoulder at 2176 cm^{-1} and the band at 2151 cm^{-1} became sharp.

There is no doubt that the two bands at 2038 and 1960 cm^{-1} can be assigned to the dechelation product (η^3-C_5Me_5)V(CO)$_4$ (1a). The presence of five CO stretching bands (1981, 1969, 1900, 1881, 1865 cm^{-1}) and three NN stretching bands (2192, 2176, 2151 cm^{-1}) indicates the formation of at least two different carbonyl dinitrogen species. Since two sets of new bands grew and reversed with constant relative intensities, it is possible to assign the bands at 2192 (ν(NN)), 1981, and 1900 cm^{-1} to (η^5-C_5Me_5)V(CO)$_3$(N_2) (1e) and those at 2176, 2151 (ν(NN)), 1969, and 1881 cm^{-1} to (η^5-C_5Me_5)V(CO)$_2$(N_2)$_2$ (1f).

The same observations were made for (η^5-C_5H_4Me)V(CO)$_4$ (2). Apart from the unsaturated ring slippage species (η^3-C_5H_4Me)V(CO)$_4$ (2a; 2055, 1981 cm^{-1}), the two substitution products (η^5-C_5H_4Me)V(CO)$_3$(N_2) (2e; 2211 (ν(NN)), 1991, 1908 cm^{-1}) and (η^5-C_5H_4Me)V(CO)$_2$(N_2)$_2$ (2f; 2190, 2182 (ν(NN)), 1962, 1872 cm^{-1}) were generated (see Table V).

The spectra of the indenyl complex (η^5-indenyl)V(CO)$_4$ (4) only showed the monosubstitution product (η^5-indenyl)V(CO)$_3$(N_2) (4e) with absorptions at 2187 (ν(NN)), 1995, 1916, and 1907 cm^{-1} on photolysis using filter A.

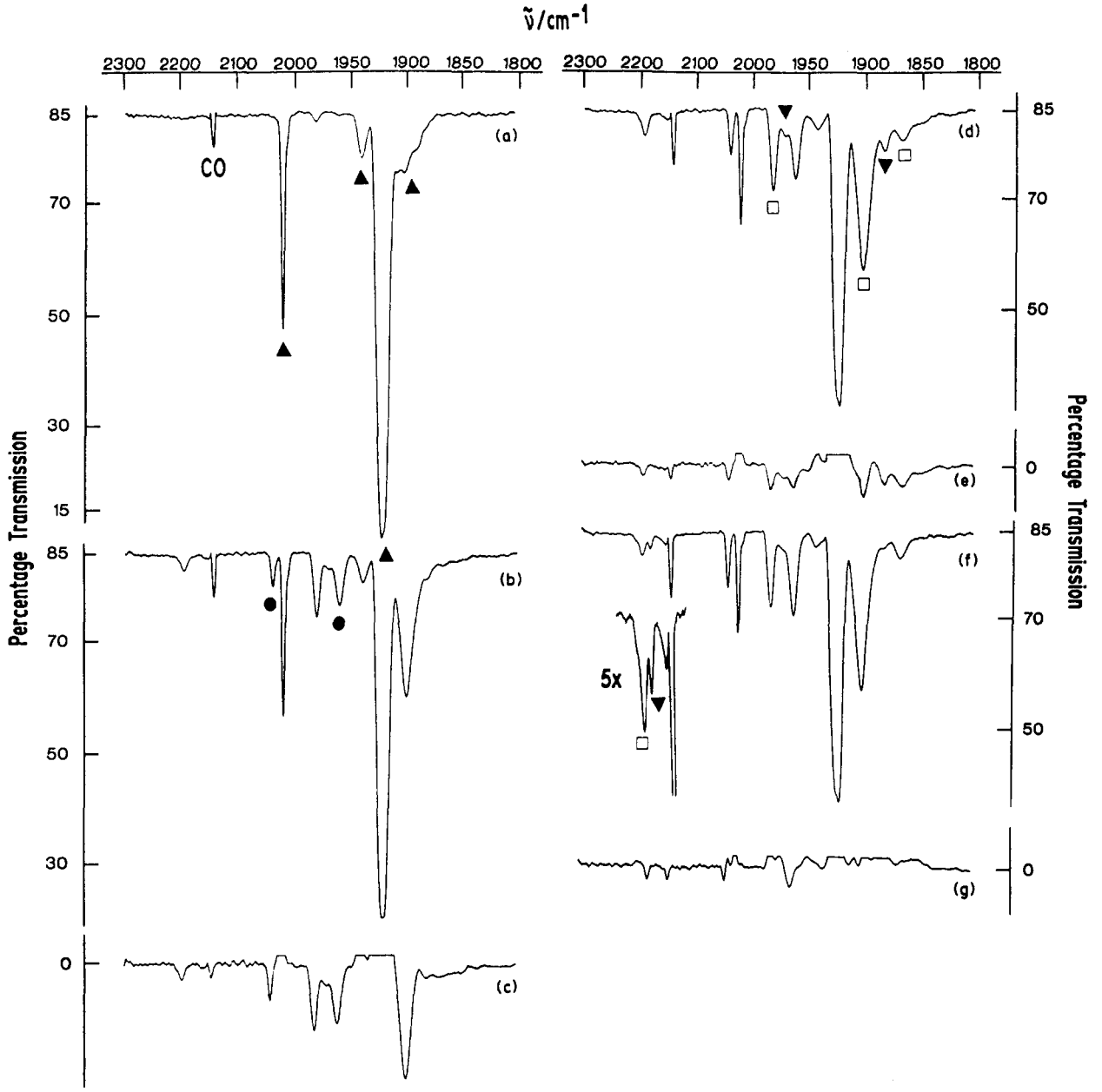

Figure 4. Infrared spectra (Perkin-Elmer 983G) from an experiment with $(\eta^5\text{-}C_5Me_5)V(CO)_4$ (**1**) isolated at high dilution in a N_2 matrix at ca. 12 K: (a) after deposition, (b) after 5-min visible irradiation (filter A), (c) difference spectrum [(b) − (a)], (d) after 3-min UV irradiation (filter B), (e) difference spectrum [(d) − (b)], (f) after 30-min visible irradiation (filter C), and (g) difference spectrum [(f) − (d)]; (▲) **1**, (●) **1a**, (□) **1e**, and (▼), **1f**.

Because of the identical behavior of the bands at 2220 (ν(NN)), 2052, and 1978 cm^{-1} on UV (filter B) and long-wavelength photolysis (filter C) (increase and decrease in intensity), they could be assigned to the compound $(\eta^3$-indenyl$)V(CO)_4(N_2)$ (**4g**), formed in ca. 5% yield. The shift to lower wavenumbers compared with $(\eta^3$-indenyl$)V(CO)_4$ (**4a**) can be explained by the slightly increased V → C back-bonding caused by the weak donor N_2. Support for this proposition comes from the fact that this species is an 18-electron complex and its ν(NN) stretching absorption is observed at relatively high wavenumbers compared with the substitution products **1e–5e**, **1f**, and **2f**.

The corresponding spectra of $(\eta^5\text{-}C_5Cl_5)V(CO)_4$ (**5**) again clearly demonstrated the photolability of this compound. In addition to the photoproducts $(\eta^3\text{-}C_5Cl_5)V(CO)_4$ (**5a**; 2077, 2035 cm^{-1}) and $(\eta^5\text{-}C_5Cl_5)V(CO)_3(N_2)$ (**5e**; 2214 (ν(NN)), 2024, 1951 cm^{-1}), the band at 2003 cm^{-1} is attributable to the dicarbonyl species $(\eta^5\text{-}C_5Cl_5)V(CO)_2$ (**5c**), which is obviously unsubstituted. The low-wavenumber band is probably obscured by the A′ band of species **5e**, and the weak absorption at 1904 cm^{-1} again demonstrates the presence of $(\eta^5\text{-}C_5Cl_5)V(CO)$ (**5d**). The appearance of shoulders for the dechelation product is suggestive for a species like $(\eta^3\text{-}C_5Cl_5)V(CO)_4(N_2)$ (**5g**; 2231 (ν(NN)), 2085, 2052 cm^{-1}), although the CO stretchings are shifted to higher wavenumbers in contrast to the observations made for $(\eta^3$-indenyl$)V(CO)_4(N_2)$ (**4g**).

By comparison with the results presented in ref 23, there are low-wavenumber terminal CO stretching bands observed for complexes **1**, **2**, **3**,[34] and **5**, which leave the identity of species responsible for those bands to be determined. Although the intensities of the absorptions are quite strong, spectral subtractions did not reveal other bands linked to those which can be observed. Since we

(34) By comparison with the results in ref 23 and the mistaken assignment in ref 22, there are bands for four unexplained species, which might indicate other photoproducts derived from the following parent complexes: 1865 cm^{-1}, $(\eta^5\text{-}C_5Me_5)V(CO)_4$; 1894 cm^{-1}, $(\eta^5\text{-}C_5H_4Me)V(CO)_4$; 1875 cm^{-1}, $(\eta^5\text{-}C_5H_5)V(CO)_4$; 1917 cm^{-1}, $(\eta^5\text{-}C_5Cl_5)V(CO)_4$.

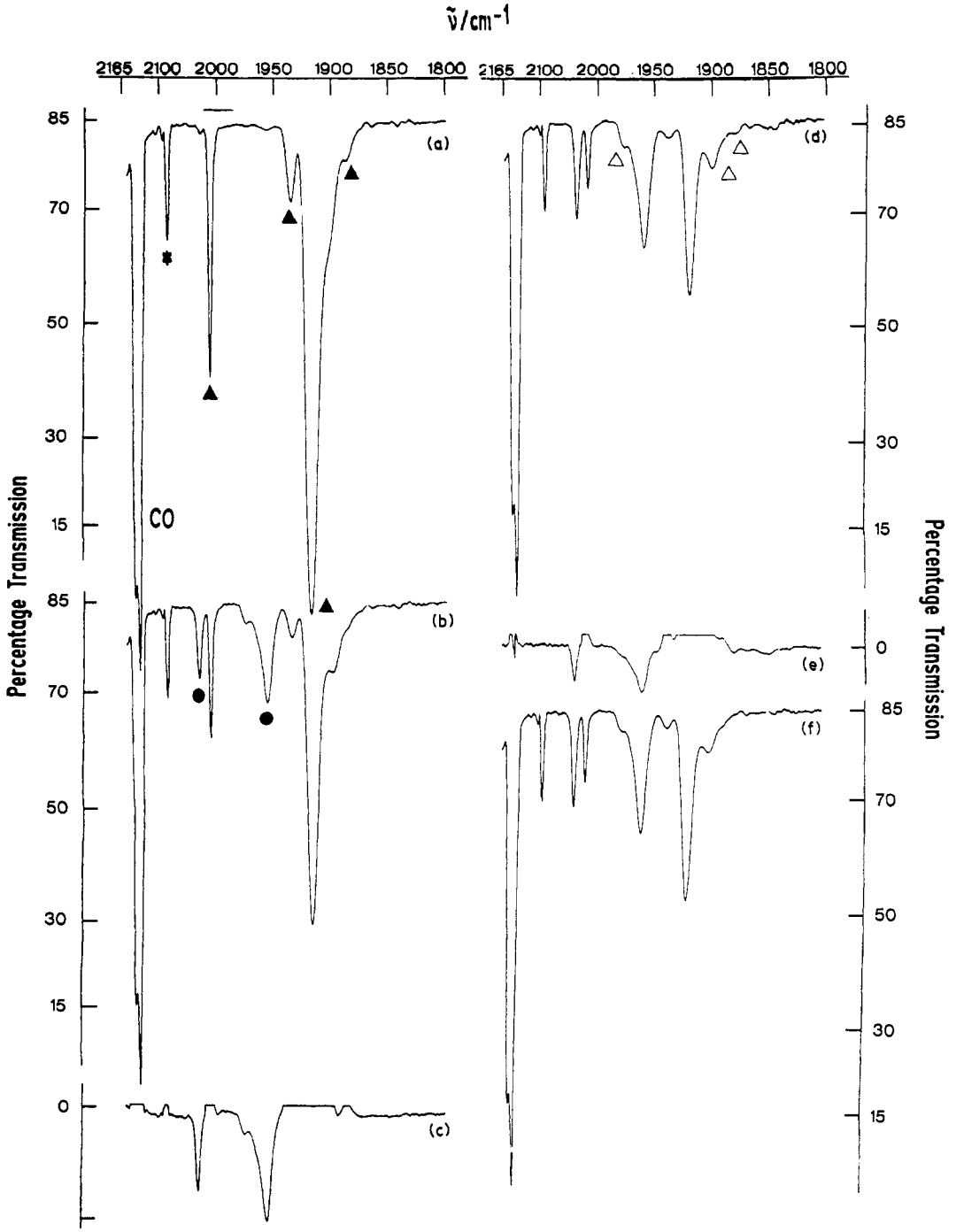

Figure 5. Infrared spectra (Perkin-Elmer 983G) from an experiment with (η^5-C_5Me_5)$V(CO)_4$ (1) isolated at high dilution in a CO matrix at ca. 12 K: (a) after deposition, (b) after 15-min visible irradiation (filter A), (c) difference spectrum [(b) – (a)], (d) after 10-min UV irradiation (filter B), (e) difference spectrum [(d) – (b)], and (f) after 30-min visible irradiation (filter C); (▲) 1, (●) **1a**, (△) **1b**, and (*) ^{13}CO in natural abundance.

can exclude dimers, it would be possible to discuss the formation of $Cp^{\#}V(CO)_2(N_2)$ species. The other bands, however, might be obscured by other absorption bands.

Photolyses of Complexes 1–5 in CO Matrices. The spectrum of (η^5-C_5Me_5)$V(CO)_4$ (1) isolated in a CO matrix (Figure 5) showed four new bands at 2037, 1979, 1959, and 1900 cm^{-1} after visible irradiation (filter A). Upon further UV irradiation (filter B), all the new bands grew in intensity and another band at 1880 cm^{-1} appeared. By comparison with the observations for the other matrix systems, these bands belong to (η^3-C_5Me_5)$V(CO)_4$ (**1a**; 2037, 1959 cm^{-1}) and (η^5-C_5Me_5)$V(CO)_3$ (**1b**; 1979, 1900, 1880 cm^{-1}). On long-wavelength irradiation (filter C), the bands of the parent complex regained intensity at the expense of the less abundant (η^5-C_5Me_5)$V(CO)_3$ (**1b**). Surprisingly there was no evidence for uptake of CO by the ring slippage species to give (η^3-C_5Me_5)$V(CO)_5$ and ultimately $V(CO)_6$.

Analogous spectra were recorded for (η^5-C_5H_4Me)$V(CO)_4$ (2) and (η^5-indenyl)$V(CO)_4$ (4) in CO matrices. For both complexes the ring slippage species **2a**, **4a**, and small amounts of the corresponding CO loss products **2b**, **4b** could be observed after UV irradiation (filter B).

The ring-halogenated complex (η^5-C_5Cl_5)$V(CO)_4$ (5) revealed the most striking behavior. After visible irradiation (filter A), and with higher intensities upon UV irradiation (filter D), the species (η^3-C_5Cl_5)$V(CO)_4$ (**5a**; 2078, 2035 cm^{-1}), (η^5-C_5Cl_5)$V(CO)_3$ (**5b**; 2029, 1947 cm^{-1}), and (η^5-C_5Cl_5)$V(CO)_2$ (**5c**; 2003, 1915 cm^{-1}) were present although in small amounts. On long-wavelength photolysis (filter

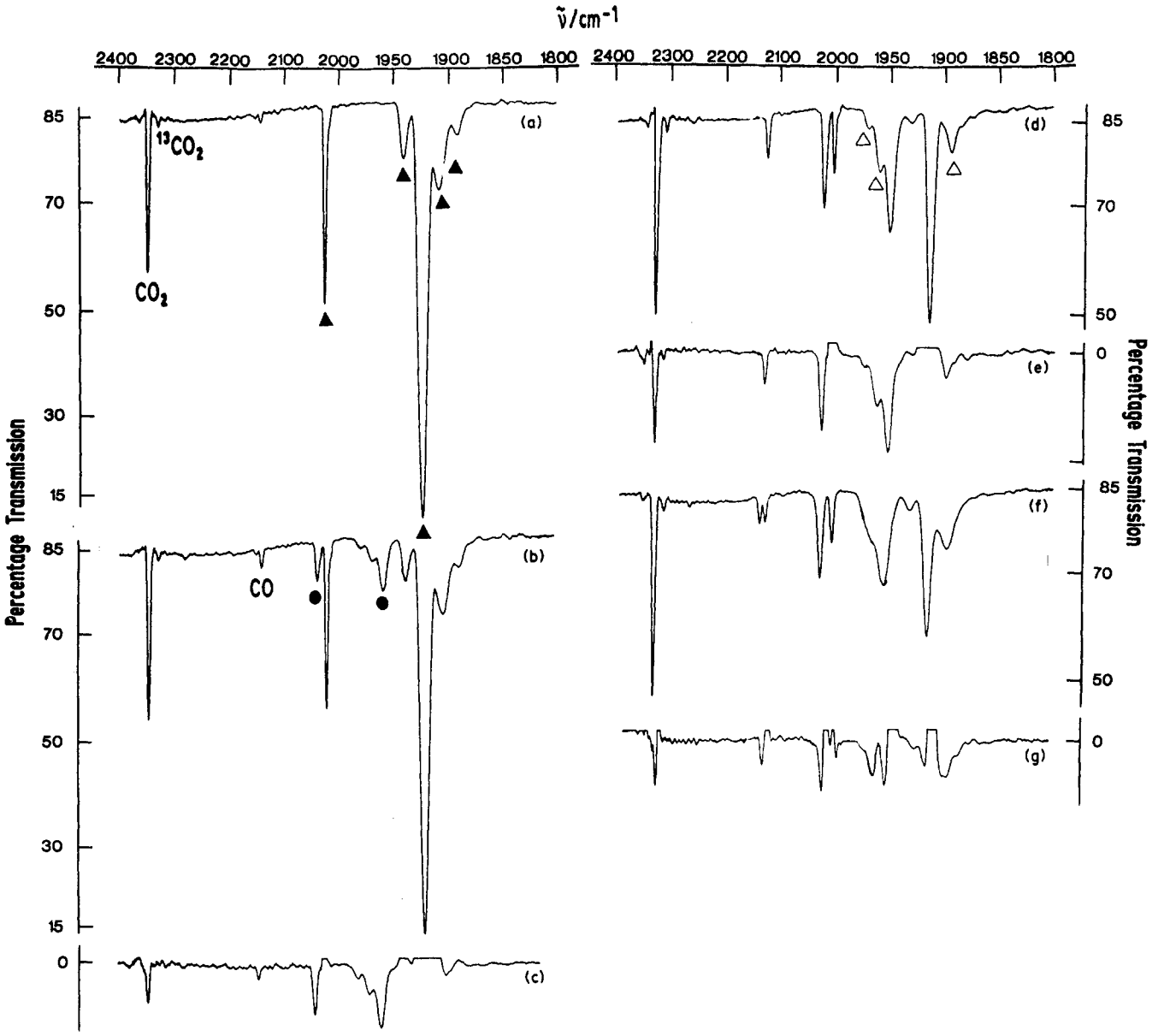

Figure 6. Infrared spectra (Perkin-Elmer 983G) from an experiment with $(\eta^5\text{-}C_5Me_5)V(CO)_4$ (1) isolated at high dilution in an O_2 matrix at ca. 12 K: (a) after deposition, (b) after 5-min visible irradiation (filter A), (c) difference spectrum [(b) − (a)], (d) after 5-min UV irradiation (filter B), (e) difference spectrum [(d) − (b)], (f) after annealing to ca. 40 K, and (g) difference spectrum [(f) − (d)]; (▲) 1, (●) 1a and, (△) 1i.

C), **5b** and **5c** decreased rapidly regenerating $(\eta^5\text{-}C_5Cl_5)V(CO)_4$ (**5**).

Photochemistry of 1 in Pure O_2 and O_2-Doped Ar Matrices. The electronic absorption spectrum of $(\eta^5\text{-}C_5Me_5)V(CO)_4$ (1) isolated at high dilution in an O_2 matrix was identical with that obtained from an Ar matrix. This indicates an absence of contact charge-transfer effects which are notable for organic, and especially aromatic, molecules.[35]

The infrared spectra of $(\eta^5\text{-}C_5Me_5)V(CO)_4$ (1), illustrated in Figure 6, showed terminal CO stretching bands at 2018 (half-width 4.2 cm^{-1}) and 1919 cm^{-1} (half-width 9 cm^{-1}). The infrared-inactive B_1 band at 1937 cm^{-1}, indicative of some deviation from strict C_{4v} symmetry, is also present together with two other absorptions at 1905 and 1888 cm^{-1} due to matrix splitting generally observed in O_2 matrices.[37] A short period of visible irradiation (filter A) led to the appearance of six new bands at 2140 (free CO), 2035, 1978, 1967, 1957, and 1900 cm^{-1}. On further UV irradiation (filter B) all the new bands increased at the expense of the parent complex.

In comparison with the results in Ar matrices, the bands at 2035 and 1957 cm^{-1} can be assigned to the dechelation product $(\eta^3\text{-}C_5Me_5)V(CO)_4$ (**1a**), while the band pattern at 1978, 1967, and 1900 cm^{-1} is indicative of a tricarbonyl species taking into account the increase of free CO during photolysis.

The spectrum in the low-wavenumber region, shown in Figure 7, exhibited a band at 935 cm^{-1}, which is typical for a side-on coordinated dioxygen complex,[37,38] although it

(35) Rest, A. J.; Salisbury, K.; Sodeau, J. R. *J. Chem. Soc., Faraday Trans. 2*, **1977**, *73*, 265.

(36) The isotopic shifts of $\nu(^{18}O_2)$ and $\nu(C^{16}O^{18}O)$ can be calculated using the following equation:[37] $\nu(^{16}O_2/^{18}O_2) = [m(^{18}O)/m(^{16}O)]^{1/2}$ where m is the relative atomic mass of the isotope. With this model the absorptions at 2346 and 935 cm^{-1} would be expected at 2278 and 881 cm^{-1}.

(37) Poliakoff, M.; Smith, K. P.; Turner, J. J.; Wilkinson, A. J. *J. Chem. Soc., Dalton Trans.* **1982**, 651.

(38) Nakamoto, K. *Infrared and Raman Spectra of Inorganic and Coordination Compounds*; 4th ed.; Wiley-Interscience: New York, 1986.

(39) Nakamura, A.; Tatsuno, Y.; Yamamoto, M.; Otsuka, S. *J. Am. Chem. Soc.* **1971**, *93*, 6052.

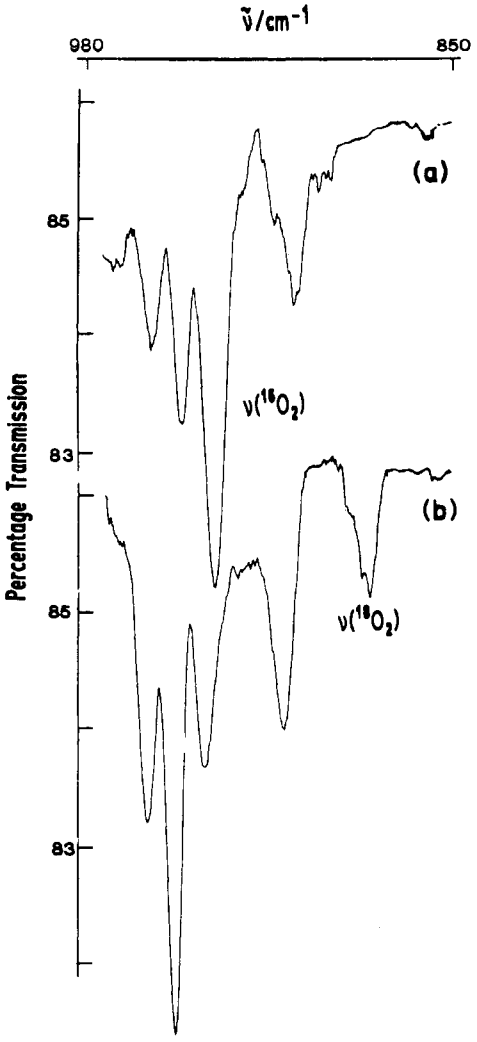

Figure 7. Infrared spectra (Perkin-Elmer 983G) from an experiment with $(\eta^5\text{-}C_5Me_5)V(CO)_4$ (1) isolated at high dilution in an O_2 matrix at ca. 12 K: (a) with $^{16}O_2$ after 5-min UV irradiation (filter B), (b) with $^{18}O_2$ after 5-min UV irradiation (filter B).

coincided with the ring skeleton vibrations of the ring slippage species as shown by the subtraction spectra.

An experiment using $^{18}O_2$ (>97%) confirmed the identity of the $\nu(O_2)$ absorption[36] and provided evidence as to whether the observed CO_2 at 2346 cm^{-1} was present due to decomposition of 1 during spray-on to prepare the matrix or formed by photooxidation of CO. As indicated in Figure 7, the new $\nu(^{18}O_2)$ band was shifted to 882 cm^{-1}, thereby confirming the assignment of the 935-cm^{-1} band to a coordinated O_2 molecule. A corresponding shift of the CO_2 absorption was not observed so that the present amount of carbon dioxide is matrix-isolated during spray-on. The increasing amount during the experiment is due to residual CO_2 on the vacuum shroud which condenses on the 12 K spectroscopic window. The change in the absorption bands compared with **1b** (1979, 1900, 1880 cm^{-1}) and **1f** (1981, 1900, 1865 cm) and the presence of the single band at 935 cm^{-1} suggested that the new complex must be $(\eta^5\text{-}C_5Me_5)V(CO)_3(\eta^2\text{-}O_2)$ (**1i**) (Table VI). The observation of a weak shoulder at 1879 cm^{-1} may be indicative of the B_1 band of a dicarbonyl species in low abundance whose A_1 band is obscured by other absorptions.

On annealing, the matrix all the new bands decreased with the exception of those assigned to the new oxo compound **1i** (in contrast to **1b** and **1f**, which decreased on annealing) and free CO, demonstrating that further reactions may be thermodynamically controlled.

Table VI. Terminal CO Stretching Band Positions (cm^{-1}) for $(\eta^5\text{-}C_5Me_5)V(CO)_4$ (1) and Its Photoproducts in O_2, O_2-Doped Ar, H_2S-Doped Ar, THF-Doped Ar, and PVC Films

complex	O_2	O_2/Ar	H_2S/Ar	THF/Ar	PVC
$(\eta^5\text{-}C_5Me_5)V(CO)_4$ (1)	2018	2017	2017	2017	2011
	1937[a]	1937[a]	1937[a]	1937[a]	1933[a]
	1919	1920	1920	1920	1903
	1905[b]	1904[b]	1905[b]	1905[b]	
	1888[b]	1888[b]	1888[b]	1888[b]	
$(\eta^3\text{-}C_5Me_5)V(CO)_4$ (1a)	2035	2037	2038	2038	2054
	1957	1959	1959	1959	1987
$(\eta^5\text{-}C_5Me_5)V(CO)_3$ (1b)			1978	1978	1964
			1900	1903	1863
			1881	1878	1843
$(\eta^5\text{-}C_5Me_5)V(CO)_3(\eta^2\text{-}O_2)$ (1i)	1978	1977			
	1967	1967			
	1900	1901			
	935[c]	936[c]			
$(\eta^5\text{-}C_5Me_5)V(CO)_3(THF)$ (1j)					*d*
					1837
					1818

[a] IR-inactive band. [b] Matrix-split band. [c] $\nu(^{16}O_2)$; $\nu(^{18}O_2)$ at 881 cm^{-1}. [d] Obscured by overlapping band of another photoproduct or low intensity due to low abundance.

The observations with oxygen-doped Ar matrices (Ar/O_2 95:5) were almost identical, but the yield of $(\eta^5\text{-}C_5Me_5)V(CO)_3(\eta^2\text{-}O_2)$ (**1i**) was not as high as in pure O_2 matrices; matrix-generated ozone[40] was not observed in the experiments.

Photochemistry of 1 and 5 in THF- and H_2S-Doped Ar Matrices. The observations made for two different dilutions (Ar/THF, Ar/H_2S 95:5 and Ar/THF 70:30, Ar/H_2S 80:20; different melting points of the dopants caused a decrease in the matrix quality) were found to be identical to those in pure Ar.

In all experiments the naked CO loss species **1b** and **5b** could be identified, and on annealing the matrices to ca. 35 K, no reactions pointing to an expected coordination of the dopants occurred. Generally S–H and $-CH_2-O-CH_2-$ vibrations are very weak, so that it was not possible to observe any absorptions of H_2S or THF in the matrix. If there had been photochemical reactions as proposed above, leading to complexes such as $Cp^*V(CO)_3(H)(SH)$ (H_2S-doped matrix) or $Cp^*V(CO)_3(THF)$ (THF-doped matrix), it would probably have been impossible to identify V–H stretching bands or changes in the $-CH_2-O-CH_2-$ vibrations. The band patterns and shifts observed for the CO-loss fragments (Table VI) are identical to those recorded for pure Ar and CH_4 matrices (Table V).

The different gas mixtures used rule out any dependence on the concentration of the dopants; the most likely conclusion which can be drawn at this stage is that the CO loss products formed upon irradiation pick up a ligand at temperatures higher than 35 K (see below).

Photochemistry of 1 in Poly(vinyl chloride) (PVC) Films. The application of polymer film media[24,41-47] has

(40) Almond, M. J.; Hahne, M. *J. Chem. Soc., Dalton Trans.* **1988**, 2255.
(41) Hooker, R. H.; Rest, A. J. *J. Organomet. Chem.* **1983**, *249*, 137.
(42) Hooker, R. H.; Rest, A. J.; Mahmoud, K. A. *J. Chem. Soc., Chem. Commun.* **1983**, 1022.
(43) Hooker, R. H.; Rest, A. J.; Mahmoud, K. A. *J. Organomet. Chem.* **1983**, *254*, C25.
(44) Hooker, R. H.; Rest, A. J. *J. Chem. Soc., Dalton Trans.* **1984**, 761.
(45) Hooker, R. H.; Rest, A. J.; Whitwell, I. *J. Organomet. Chem.* **1984**, *266*, C27.
(46) Hooker, R. H.; Rest, A. J. *J. Chem. Soc., Dalton Trans.* **1990**, 1231.
(47) Hooker, R. H.; Rest, A. J.; Mahmoud, K. A. *J. Chem. Soc., Dalton Trans.* **1990**, 1231.

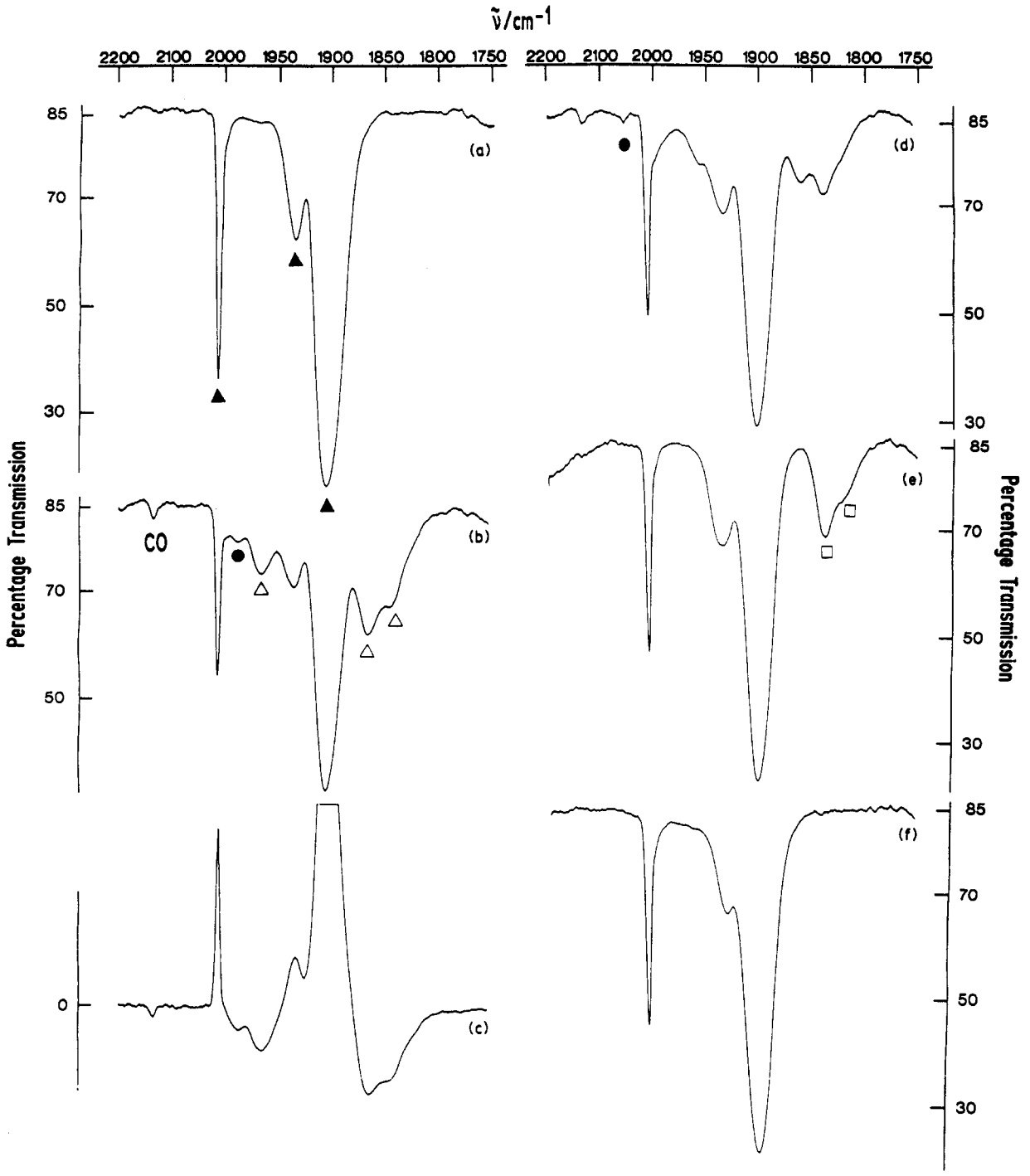

Figure 8. Infrared spectra (Perkin-Elmer 983G) from an experiment with (η^5-C_5Me_5)$V(CO)_4$ (1) isolated at high dilution in a polymer film (PVC) at ca. 12 K: (a) after deposition, (b) after 20-min UV irradiation (filter B), (c) difference spectrum [(b) − (a)], (d) after annealing for 15 min, (e) after annealing for 150 min, and (f) after annealing for 300 min; (▲) 1, (●) **1a**, (△) **1b**, and (□) **1j**.

enabled the thermal reactivity of unstable species to be monitored over wide temperature ranges. These polymer films behave analogously to gas matrices at ca. 12 K and can also be employed for studying involatile complexes. One most important fact is that the residual casting solvent (THF), typically present in amounts of ca. 8%, can react with unsaturated species, thus forming compounds like Cp*$V(CO)_3$(THF). Experiments were carried out with (η^5-C_5Me_5)$V(CO)_4$ (1), isolated at high dilution (1:1000) in a PVC polymer film.

The infrared spectra of 1, illustrated in Figure 8, showed two absorptions at 2011 and 1903 cm^{-1} (half-widths 12 and 35 cm^{-1}, respectively), expected for a C_{4v} symmetry of the $V(CO)_4$ moiety. The band at 1933 cm^{-1} is indicative of a distortion of the ideal C_{4v} symmetry. The half-widths are about twice as large as those observed in an Ar matrix and reveal the "site effect" in the polymer film, where splitting bands or shoulders are normally not resolved. After 20-min UV irradiation (filter B) five new bands emerged at 2133 (free CO), 1987, 1964, 1863, and 1843 cm^{-1}. In comparison with the experiments in gas matrices, the three bands at lower wavenumbers can be assigned to (η^5-C_5Me_5)$V(CO)_3$ (**1b**; 1964, 1863, 1843 cm^{-1}) whereas the high wavenumber absorption at 1987 cm^{-1} seems to be the E band of (η^3-C_5Me_5)$V(CO)_4$ (**1a**). On annealing the polymer film for 15 min, all the new bands decreased in intensity regenerating the parent complex, and a new band grew at ca. 1840 cm^{-1}. A weak absorption at 2054 cm^{-1} may be in-

Table VII. Decreasing Amount of $(\eta^5\text{-}C_5Me_5)V(CO)_3(THF)$ (1j) on Annealing the PVC Film

annealing time (min)	integral	rel intensity (%)
150	2.21	100
200	1.70	77
250	0.18	8
300	0.0	0

Scheme I. Photochemical Reactions[a] of $(\eta^5\text{-}C_5Me_5)V(CO)_4$ (1)[a]

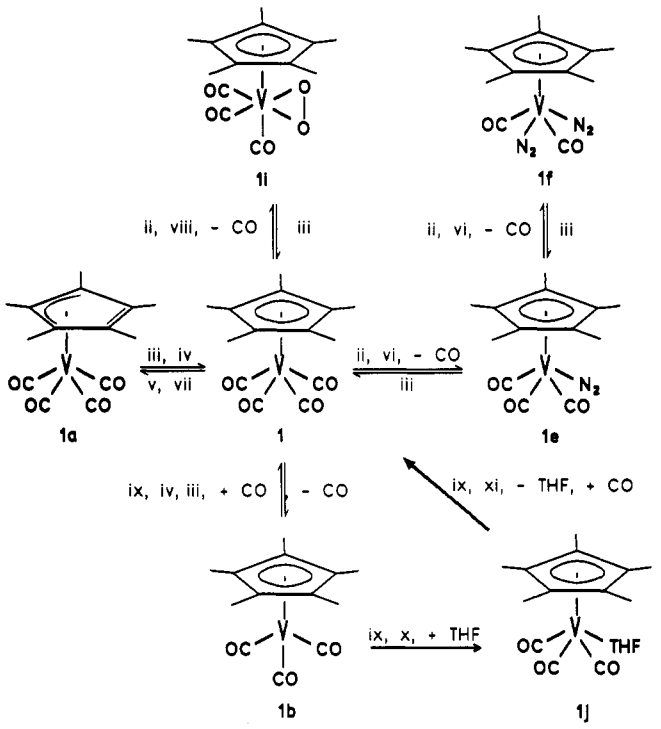

[a] Conditions: (i) Ar, CH_4; (ii) UV irradiation (filter B); (iii) visible irradiation (filter C); (iv) annealing; (v) visible irradiation (filter A); (vi) N_2; (vii) Ar, CH_4, N_2, or CO; (viii) O_2, O_2-doped Ar; (ix) PVC film; (x) annealing for 150 min; (xi) annealing for 300 min.

dicative of the A_1 band of **1a**. After annealing for a further 135 min (totally 150 min), the bands for **1b** vanished and the absorption at 1837 cm^{-1} together with a shoulder at 1818 cm^{-1} revealed a maximum amount of the new complex. Since the film contained residual casting solvent (THF) in a rather high amount (ca. 4–8%), a new species which is likely to be present is $(\eta^5\text{-}C_5Me_5)V(CO)_3(THF)$ (**1j**, for which bands occur in THF solution at 1937, 1820 cm^{-1} [19]). The low-wavenumber band in the PVC film at 1818 cm^{-1} correlates well with the lower band in THF solution, but the higher A′ band in PVC is obscured by a band of $(\eta^5\text{-}C_5Me_5)V(CO)_4$ (**1**). The thermal behavior of the new species which decomposes as the film warms up, is consistent with the behavior of $Cp^*V(CO)_3(THF)$ (Table VI), which decomposes in solution above 270 K.[19]

The decrease of the amount of **1j** on annealing (1 min ~0.8 K) in favor of the parent complex is demonstrated in Table VII using the integrals of the absorption bands.

Discussion

The photochemical reactions of the half-sandwich complexes **1**, **2**, **4**, and **5** in frozen gas matrices at ca. 12 K are summarized in the scheme for $(\eta^5\text{-}C_5Me_5)V(CO)_4$, (**1**), as the representation for the complexes **1–5**. The results may be compared with the previous ones obtained for $(\eta^5\text{-}C_5H_5)V(CO)_4$ (**3**).[22]

Photolyses with visible radiation in all matrices primarily resulted in the formation of unsaturated ring slippage species $(\eta^3\text{-}Cp^\#)V(CO)_4$ (**1a–5a**), while irradiation with high-energy UV light caused ejection of CO ligands from the parent complexes yielding coordinatively unsaturated intermediates $(\eta^5\text{-}Cp^\#)V(CO)_n$ (n = 1–3; **1b–5b**; **2c**, **3c**, **5c**; **3d**, **5d**), depending on the degree of ring substitution with either donor or acceptor substituents. The reactivity of these intermediates was demonstrated thermally (by annealing) and photochemically (by carrying out the experiments in the presence of potential ligands, i.e., in N_2 and CO matrices) to give **1e–5e**; **1f**, **2f**; **4g**, **5g**; and **3h**.

Table VIII. Relative Intensities of the CO Stretching Bands and Calculated Bond Angles of the Dicarbonyl Complexes 1f, 2c, 2f, and 5c in Different Matrix Gases

complex	matrix gas	I_{asym}	I_{sym}	calcd ∠OC–V–CO (deg)
$(\eta^5\text{-}C_5Me_5)V(CO)_2(N_2)_2$ (**1f**)	N_2	3.26	1.70	108.3
		4.00	2.64	101.8[a]
$(\eta^5\text{-}C_5H_4Me)V(CO)_2$ (**2c**)	Ar	1.45	1.15	96.6
	CH_4	1.24	0.96	97.4
$(\eta^5\text{-}C_5H_4Me)V(CO)_2(N_2)_2$ (**2f**)	N_2	1.34	0.93	100.2
		8.99	6.62	98.8[a]
$(\eta^5\text{-}C_5Cl_5)V(CO)_2$ (**5c**)	Ar	1.29	1.10	94.7
	CH_4	0.89	0.85	91.2
	CO	1.80	1.43	96.6

[a] Calculated angle N_2–V–N_2.

The typical photoreactions of $(\eta^5\text{-}C_5Me_5)V(CO)_4$ (**1**) are shown in the scheme. The formation of the unsaturated ring slippage species **1a** upon visible irradiation is similar to that observed for **3a**.[22] However, the bands for **3a** were found to be shifted to lower wavenumbers. In order to discuss the influence of a dechelation process on the CO absorption bands, the region of the ring skeleton vibrations was recorded for **1a**, which could be obtained in high yields. The shift of the CO stretching absorptions to higher wavenumbers and the concomitant appearance of three new bands at 955, 946, and 935 cm^{-1} in the ring-skeleton region at lower wavenumbers, as compared with the single absorption at 1034 cm^{-1} for the parent complex **1**, can be ascribed to the decreased electron density of the metal center, the decreased back-bonding, and the electronic distortion of the ring ligand. Photolysis with UV light resulted in the formation of the tricarbonyl species **1b**, which regenerated the parent complex either thermally (after annealing) or photochemically (after visible irradiation).

In nitrogen matrices the mono- and bis(dinitrogen) complexes **1e** and **1f** were generated. The observation of the bis(dinitrogen) complex for **1** and also for **2** is in contrast to the mono(dinitrogen) complexes observed for **3**, **4**, and **5**. The relative intensities of the symmetric (I_{symm}) and antisymmetric ($I_{antisymm}$) terminal CO and NN stretching bands were used to calculate bond angles using the expression[48]

$$I_{antisymm}/I_{symm} = \tan^2(\theta/2)$$

The values obtained (∠OC–V–CO = 108.3° and ∠NN–V–NN = 101.8°; Table VIII) are more consistent with a trans geometry than a cis geometry.

The photochemical reactions of $(\eta^5\text{-}C_5H_4Me)V(CO)_4$ (**2**) are very similar to those of **1**, with one exception: irradiation with UV light in Ar and CH_4 matrices yielded not only **2b** but also the dicarbonyl species **2c**. The calculated bond angles of 96.6° (Ar) and 97.4° (CH_4) indicated a planar geometry of the metal dicarbonyl moiety. The formation of **2e** and *trans*-**2f** in N_2 matrices was similar to the generation of **1e** and **1f**.

(48) Braterman, P. S. *Metal Carbonyl Spectra*; Academic Press: London, 1975.

At this stage of the discussion it is useful to mention the results obtained for the unsubstituted complex, $CpV(CO)_4$ (**3**).[22] In CH_4 matrices all CO loss species were observed, i.e., **3b–3d**, while in N_2 matrices **3e** was the only substitution product obtained. The mono(dinitrogen) complex, **3e**, has also been formed in liquid Xe at −78 °C either by photolysis of **3** or by the displacement of H_2 from $(\eta^5\text{-}C_5H_5)V(CO)_3(H_2)$ by N_2.[23,49]

In contrast to the experiments in CO matrices, a $(\eta^3\text{-}C_5H_5)V(CO)_5$ species **3h** was also identified. The general trend of ring substitution with methyl groups (donor ligands) seems to stabilize bis(dinitrogen) complexes **1f** and **2f** and lead to the preferred formation of the dechelation products **1a** and **2a**, while monocarbonyl species **1d** and **2d** were not observed and only one dicarbonyl complex **2c** was present in low abundance.

The photochemical reactions of $(\eta^5\text{-indenyl})V(CO)_4$ (**4**) show a kind of intermediate behavior. The benzo-anellated cyclopentadienyl ring of this half-sandwich complex acts as a weak acceptor ligand. The formation of **4b** is more similar to the behavior of complexes **1** and **2**, but the reactions in N_2 matrices, yielding **4e**, are comparable with those of the unsubstituted complex **3**. The presence of two isomers for the dechelation product **4a** and **4a′** and the appearance of the 18-electron species $(\eta^3\text{-indenyl})V(CO)_4(N_2)$ (**4g**) are the most striking results observed for **4**.

The photochemistry of the ring-halogenated half-sandwich complex $(\eta^5\text{-}C_5Cl_5)V(CO)_4$ (**5**) is dominated by dissociative loss of CO. Even after visible irradiation, the species **5b–5d** can be identified in Ar and CH_4 matrices. The presence of the unsaturated complexes **5b** and **5c** in CO matrices after UV irradiation, although in low abundance, emphasizes the high reactivity of **5**. The planar geometry of **5c** was assigned on the basis of the calculated OC–V–CO bond angles of $\Theta = 94.7°$ (Ar), 91.2° (CH_4), and 96.6° (CO). One band of the CO loss species **5c** can also be observed in N_2 matrices, but there is only one substitution product, **5e**. The unsaturated ring slippage species **5a** appeared in all matrices, but in low abundance compared with **1a** and **2a**.

The observation of the 18-electron species $(\eta^3\text{-}C_5Cl_5)V(CO)_4(N_2)$ (**5g**) in N_2 matrices is consistent with the reaction pathways of half-sandwich complexes with acceptor substituents attached to the cyclopentadienyl ring (cf. **4g**). Such complexes tend to eject CO ligands because the electron density at the metal center is low. The easy loss of CO from **5** opens new possibilities for photochemically induced chalcogen reactions at ambient temperatures.

The high amounts of the dechelation products **1a** and **2a** suggest a possible contribution of S_N2 pathways in solution:

$$(\eta^5\text{-}C_5Me_5)V(CO)_4 \xrightarrow{h\nu} (\eta^3\text{-}C_5Me_5)V(CO)_4 \quad (9)$$
1 **1a**

$$(\eta^3\text{-}C_5Me_5)V(CO)_4 + L \rightarrow (\eta^3\text{-}C_5Me_5)V(CO)_4(L) \quad (10)$$
1a

$$(\eta^3\text{-}C_5Me_5)V(CO)_4(L) \rightarrow (\eta^5\text{-}C_5Me_5)V(CO)_3(L) + CO \quad (11)$$

The photochemistry of $(\eta^5\text{-}C_5Me_5)V(CO)_4$ (**1**) in pure O_2 and O_2-doped Ar matrices is consistent with that reported for $M(CO)_6$ complexes (M = Cr, Mo, and W), where $M(O_2)(CO)_2$ (M = Cr, Mo, and W), $M(O_2)(CO)_4$ (M = Cr, Mo, and W), MO_2 (M = Cr), and MO_3 (M = Mo and W) species were observed.[37,40,50–52] In the latter experiments formation of O_3 (1040, 1032, 702 cm)[40] and CO_2,[37] the oxidation product of the carbonyl ligand, occurred because of the prolonged broad-band UV–visible irradiation. In the experiments with **1** using short irradiation times, no CO_2 and O_3 were detected. The side-on bonding of the O_2 ligand in **1i** is supported by $^{18}O_2$ studies.

The unexpectedly low concentration of the dechelation product $(\eta^3\text{-}C_5Me_5)V(CO)_4$ (**1a**) in PVC films can probably be rationalized on the basis of the matrix "cage" rather than any photophysical process since Ar and Cl are adjacent to each other and might exert similar "heavy atom" effects. The packing of Ar and other gas molecules around substrate molecules affords a "tight cage" whereas that afforded by PVC is much more amorphous so as to produce a "loose cage". Loose cage processes leading to the ejection of a ligand, e.g., CO, will be enhanced over those for a tight cage since the ejected ligand, which might readily recombine, will be further from the metal center. For example, $(\eta^5\text{-}C_5H_5)Fe(CO)(CH_3)$ was observed on photolysis of $(\eta^5\text{-}C_5H_5)Fe(CO)_2(CH_3)$ in PVC but not in gas matrices.[53]

Conclusions. The results described in this work bear out those of a previous study[22] that ring dechelation/ring slippage pathways may play a significant part in the thermal and photochemical reactions of ring– and substituted–ring–metal complexes such that existing and future mechanistic studies should take seriously such processes.

Acknowledgment. We thank the S.E.R.C. for support (to A.J.R.), the Deutsche Forschungsgemeinschaft and the Fonds der Chemischen Industrie for grants (to M.H.), and the Deutsche Akademische Austauschdienst for a Short-Term Fellowship (to M.S.).

OM920376O

(49) The band positions for **3e** in liquid Xe (2199.5 (ν_{NN}), 1995.2, 1915.4, 1911.4 cm^{-1}), were highlighted[23] as different from those quoted for N_2 matrices (2210.3 (ν_{NN}), 1995.6, 1911.9, 1875.1 cm^{-1}).[22] Upon close examination of the N_2 matrix spectra it is clear that the lower band at 1875.1 cm^{-1} does not correlate with the set of bands at 2210.3, 1995.6, and 1911.9 cm^{-1} (matrix split band) so that there is indeed agreement between N_2 matrix and liquid Xe experiments.

(50) Almond, M. J.; Crayston, J. A.; Downs, A. J.; Poliakoff, M.; Turner, J. J. *Inorg. Chem.* **1986**, *25*, 19.
(51) Almond, M. J.; Downs, A. J. *J. Chem. Soc., Dalton Trans.* **1988**, 809.
(52) Almond, M. J.; Downs, A. J.; Perutz, R. N. *Inorg. Chem.* **1985**, *24*, 275.
(53) Hooker, R. H.; Rest, A. J.; Whitwell, I. *J. Organomet. Chem.* **1984**, *266*, C27.